

Global Frequency Reference Tracking as an Oscillation Suppression Mechanism in VSM Primary Control: A Coupled-Oscillator Study

Taha Saeed Khan, *Student Member, IEEE,*

Abstract—Synchronization in power systems is traditionally achieved through physical network coupling, whereby inverter-based resources (IBRs) and synchronous machines converge to a common frequency via oscillatory swing dynamics. In conventional operation, secondary control acts on a slow time scale and is typically engaged only after the primary dynamics have largely settled. As a result, in the absence of an explicit global reference, disturbances can induce prolonged transients and large phase excursions.

This work considers a setting in which the total active power balance is known and maintained at all times, and proposes a control architecture for virtual synchronous machine (VSM) based inverters in which all units track a broadcast global frequency reference. Under this assumption, synchronization is transformed from a mutual oscillator-locking problem into a reference-tracking problem.

Using a second-order swing-network model, we show that embedding a simple proportional-integral (PI) frequency controller can significantly improve transient behavior. A washout mechanism ensures that the additional control action vanishes in steady state, thereby preserving network-determined power sharing. Simulations on a three-oscillator network demonstrate reduced frequency overshoot, elimination of underdamped oscillations, and lower angular stress compared to conventional open-loop synchronization, highlighting the effectiveness of a global frequency reference as a coordination mechanism for grid-forming inverter networks.

Index Terms—Grid-forming inverters, synchronous rotating frame, global frequency reference, frequency control, Kuramoto oscillators, non-oscillatory synchronization.

I. INTRODUCTION

The synchronization of generator clusters in power systems has traditionally been analyzed through absolute rotor-angle and frequency dynamics [1]. In both synchronous-machine-dominated grids and modern inverter-dominated systems, frequency emerges as a collective variable governed by the balance between power injections, network coupling, inertia, and damping. In the absence of an explicit global reference, synchronization is achieved implicitly through physical interactions among generators, leading to oscillatory transient behavior following disturbances [2].

When analyzed in a stationary coordinate system, any disturbance such as during faults, generator tripping, or load changes, frequency restoration relies on large rotor-angle excursions and prolonged inter-area oscillations [3], which

Taha Saeed Khan is with the School of Electrical Computer Engineering, Oklahoma State University, Stillwater 74075, OK, USA

impose significant stress on machines, converters, and network components.

Unlike synchronous machines, a cluster of Grid forming (GFM) IBRs are capable of establishing voltage and frequency autonomously, but they still rely predominantly on local power-frequency feedback and physical coupling through the network to achieve synchronization. Consequently, even with advanced control structures, frequency regulation remains fundamentally an oscillatory synchronization problem which experience similar challenges as faced by conventional synchronous machines [4].

Although inverter-based resources (IBRs), particularly grid-forming inverters, are inherently more capable than synchronous machines in autonomously establishing voltage and frequency, they still predominantly rely on conventional generator-like mechanisms—namely local power-frequency feedback and physical network coupling—for synchronization. Consequently, even with advanced GFM control architectures, frequency regulation remains fundamentally an oscillatory synchronization process unless augmented by an explicit reference or secondary coordination layer [5].

In this work, we consider a setting in which the aggregate active power balance is perfectly known, i.e., total generation equals total consumption at all times. In modern power systems, this assumption is increasingly realistic [6] due to high-resolution measurement, fast communication, and active energy management systems that can estimate system-wide power demand and adjust the active power setpoints of inverter-based resources (IBRs) within sub-second duration. Under this assumption, global frequency drift caused by net power imbalance is eliminated, allowing the analysis to focus exclusively on synchronization and transient dynamics. Building on this premise, a control architecture is proposed in which all grid-forming resources track a broadcast global frequency reference. Hence, by embedding the system dynamics in a synchronous rotating reference frame, the synchronization problem is transformed from mutual oscillator locking into a reference-tracking task.

This change in perspective has important consequences. Rather than relying on network-induced oscillations to redistribute power, frequency deviations can be directly regulated through simple modified primary control actions. As shown in this paper, augmenting standard grid-forming dynamics with a proportional-integral (PI) controller acting on frequency deviation enables fast, non-oscillatory convergence to equilibrium. A washout mechanism [7] is employed to ensure that the

control action vanishes at steady state, thereby preserving the natural power-flow solution and network-determined power sharing.

The remainder of this paper formalizes these ideas using a second-order Kuramoto (swing-network) model, which provides a compact and physically interpretable abstraction of VSM based inverter synchronization. Through numerical simulations, it is demonstrated that how the introduction of a global frequency reference fundamentally can alter the transient behavior of grid-forming networks, yielding improved damping, reduced frequency overshoot, and significantly smaller angular excursions.

II. GRID-FORMING (GFM) INVERTERS FREQUENCY CONTROL: THREE CANONICAL LAWS

In practical grid-forming inverters, the frequency variable is generated internally and evolves according to a chosen grid-forming law. The three most common families are: (i) droop-based grid forming [8], (ii) virtual synchronous machine (VSM) [9], and (iii) oscillator-based methods such as dispatchable virtual oscillator control (dVOC) [10] or matching-control-type oscillators. Below equations provides a representative summary for each class.

1) *Droop-Based Grid-Forming Control*: Droop control implements an algebraic power-frequency relation:

$$\omega_i(t) = \omega_0 - m_{p,i}(P_i(t) - P_i^*), \quad (1)$$

where ω_0 is the nominal angular frequency, $m_{p,i} > 0$ is the active-power droop coefficient, $P_i(t)$ is the measured active power injection, and P_i^* is the active power setpoint. Equivalently, the phase angle is obtained by integration:

$$\dot{\theta}_i(t) = \omega_i(t). \quad (2)$$

Key Property: Droop generally permits a nonzero steady-state frequency deviation when $P_i(t) \neq P_i^*$.

2) *Virtual Synchronous Machine (VSM) / Swing Emulation*: VSM control embeds frequency in a first-principles-like inertial law:

$$M_i \dot{\omega}_i(t) + D_i(\omega_i(t) - \omega_0) = P_i^* - P_i(t), \quad (3)$$

$$\dot{\theta}_i(t) = \omega_i(t), \quad (4)$$

where $M_i > 0$ is a virtual inertia constant and $D_i > 0$ is a damping coefficient.

Key Property: Frequency dynamics are inertial (second-order in θ_i), improving transient behavior, but a secondary layer is needed to converge to reference frequency.

3) *Oscillator-Based Grid Forming (e.g., dVOC / Matching Type)*: Oscillator-based GFM methods generate an internally stable limit cycle and synchronize through feedback. A generic complex-oscillator form can be written as:

$$\dot{v}_{\alpha\beta,i}(t) = \omega_0 J v_{\alpha\beta,i}(t) + \kappa_i (v_{\alpha\beta,i}^*(t) - v_{\alpha\beta,i}(t)) + \Psi_i(P_i(t), Q_i(t)), \quad (5)$$

where $v_{\alpha\beta,i} \in \mathbb{R}^2$ is the voltage vector in the stationary $\alpha\beta$ frame, $J = \begin{bmatrix} 0 & -1 \\ 1 & 0 \end{bmatrix}$ is the 90° rotation matrix,

$\kappa_i > 0$ is a synchronization gain, $v_{\alpha\beta,i}^*$ is a voltage reference (magnitude/phase objective), and $\Psi_i(\cdot)$ denotes the power-based feedback that enforces desired P - Q behavior. One may also express the oscillator in polar coordinates $v_{\alpha\beta,i} = V_i [\cos \theta_i, \sin \theta_i]^\top$, yielding an implicit frequency evolution through $\dot{\theta}_i$.

Key Property: Frequency emerges from the oscillator dynamics and power-based feedback.. This is the only control where reference frequency appears in primary control.

As explicit in the case of VSM, the applied control law inherently permit frequency deviations following disturbances, unless a secondary control mechanism, analogous to Automatic Generation Control (AGC) in synchronous generating units is activated.

However, IBRs control operates on significantly faster time scales and does not necessarily require a distinct secondary control layer. Instead, the frequency-restoration functionality can be embedded directly within the primary grid-forming controller. This integration can significantly improve transient performance and mitigate oscillatory behavior.

To explicitly drive frequency deviations to zero, the primary grid-forming control law can be augmented with a frequency-tracking loop:

This paper demonstrates that incorporating reference frequency tracking within the primary control layer is a key enabling mechanism for improving frequency regulation using simple Proportional–Integral (PI) control laws.

III. GENERATOR AS 2nd ORDER KURAMOTO OSCILLATOR

The classical swing equation provides the foundational dynamic model emulated by VSM-based controllers for power-system synchronization. For a conventional synchronous generator, the dynamics can be written as follows.

Let δ_i denote the electrical rotor angle of generator i , and define the synchronous reference frame $\theta_i := \delta_i - \omega_s t$, where ω_s is the nominal synchronous speed. Then $\dot{\theta}_i = \omega_i - \omega_s$.

The classical swing equation is

$$M_i \ddot{\omega}_i + D_i(\omega_i - \omega_s) = P_{m,i} - P_{e,i}, \quad (6)$$

where M_i and D_i denote inertia and damping, and $P_{m,i}$ and $P_{e,i}$ are mechanical and electrical powers, respectively. The swing equation states that the rotor accelerates or decelerates according to the imbalance between mechanical input power and electrical output power, filtered by inertia and damping.

Under a balanced positive-sequence network model, the electrical power injection can be written as

$$P_{e,i} = \sum_{j=1}^N V_i V_j (G_{ij} \cos(\theta_i - \theta_j) + B_{ij} \sin(\theta_i - \theta_j)). \quad (7)$$

Assuming a lossless (or weakly resistive) network ($G_{ij} \approx 0$) and approximately constant voltage magnitudes, (7) reduces to the sinusoidal coupling form

$$P_{e,i} \approx \sum_{j=1}^N K_{ij} \sin(\theta_i - \theta_j), \quad K_{ij} := V_i V_j B_{ij}. \quad (8)$$

Substituting (8) into (6) and expressing the dynamics in the synchronous frame yields the second-order Kuramoto (swing-network) model

$$M_i \ddot{\theta}_i + D_i \dot{\theta}_i = P_{m,i} - \sum_{j=1}^N K_{ij} \sin(\theta_i - \theta_j). \quad (9)$$

IV. THREE-GENERATOR INERTIAL KURAMOTO

A. Swing-network dynamics

Three coupled generators using the inertial Kuramoto (swing-network) model in a synchronous rotating frame are simulated. Let $\theta_i(t)$ denote the phase angle of generator i and $\omega_i(t) = \dot{\theta}_i(t)$ denote its frequency deviation. The dynamics are:

$$\dot{\theta}_i = \omega_i, \quad (10)$$

$$M_i \dot{\omega}_i + D_i \omega_i = P_i(t) - \sum_{j=1}^N K_{ij} \sin(\theta_i - \theta_j), \quad i = 1, \dots, N, \quad (11)$$

where $M_i > 0$ and $D_i > 0$ represent inertia and damping, respectively.

$$K_{ij} = \begin{cases} K_0, & i \neq j, \\ 0, & i = j. \end{cases} \quad (12)$$

B. Step disturbance with power balance

A step disturbance is applied to the mechanical power inputs at time t_0 :

$$P(t) = P_{\text{base}} + u(t - t_0) P_{\text{step}}, \quad (13)$$

where $u(\cdot)$ is the unit-step function.

To ensure that the disturbance excites only relative (inter-area) dynamics and does not induce a spurious acceleration of the system's center-of-inertia (COI) mode, the mechanical power inputs are constructed to be power-balanced at all times.

First, a baseline mechanical power vector $\mathbf{P}_{\text{base}} \in \mathbb{R}^N$ is selected such that

$$\mathbf{1}^\top \mathbf{P}_{\text{base}} = \sum_{i=1}^N P_{\text{base},i} = 0, \quad (14)$$

which guarantees that, prior to the disturbance, the net mechanical torque applied to the system is zero. Consequently, the synchronous (COI) frequency remains constant and no global acceleration is present.

Next, a step disturbance vector $\mathbf{P}_{\text{step}} \in \mathbb{R}^N$ is constructed by applying a power increment to a selected generator and then removing its mean value, enforcing

$$\mathbf{1}^\top \mathbf{P}_{\text{step}} = \sum_{i=1}^N P_{\text{step},i} = 0. \quad (15)$$

This normalization ensures that the step disturbance redistributes power among generators without altering the total mechanical input. As a result, the disturbance excites only the relative swing modes of the system rather than the COI mode. Without this constraint, the system would experience a net

torque imbalance, leading to a uniform drift of all frequencies and obscuring synchronization behavior.

All simulations are performed in a synchronous rotating reference frame; hence, ω_i denotes frequency deviation from the nominal value, and $\omega_i = 0$ corresponds to operation at the rated 60 Hz frequency.

C. Equilibrium-consistent initial conditions

To initiate the simulation from a synchronized steady-state operating point (a “flat start” in frequency), we set the initial frequency deviations to zero:

$$\omega(0) = \mathbf{0}. \quad (16)$$

The initial phase angles $\theta(0) = \theta_0$ are computed as the steady-state solution to the open-loop power-balance equations under the baseline mechanical power P_{base} :

$$P_{\text{base},i} - \sum_{j=1}^N K_{ij} \sin(\theta_{0,i} - \theta_{0,j}) = 0, \quad i = 1, \dots, N. \quad (17)$$

In the numerical implementation, this nonlinear system of equations is solved using the `fsolve` algorithm in Matlab [11] to ensure that $\dot{\omega}(0) = 0$, thereby preventing initial spurious transients prior to the applied disturbance.

D. Center of inertia as relative reference

To remove the arbitrary global phase reference, relative angles are computed via the COI angle

$$\theta_{\text{COI}}(t) := \frac{\sum_{i=1}^N M_i \theta_i(t)}{\sum_{i=1}^N M_i}, \quad \theta_i^{\text{rel}}(t) := \theta_i(t) - \theta_{\text{COI}}(t). \quad (18)$$

V. THREE-GENERATOR INERTIAL KURAMOTO WITH REFERENCE-TRACKING PI

An explicit global frequency setpoint ω_{ref} is used in this case where again a network of three inertial Kuramoto is simulated. Let $\phi_i(t)$ denote the phase angle of generator i in this rotating frame, and let $\Delta\omega_i(t)$ denote the frequency deviation from ω_{ref} . This converts synchronization from an open-loop “mutual locking” problem into a *tracking* problem where $\Delta\omega_i \rightarrow 0$ is directly enforced.

A. Closed-loop swing-network dynamics

The inertial Kuramoto (swing-network) model with all-to-all coupling is

$$\dot{\phi}_i = \Delta\omega_i, \quad i = 1, \dots, N, \quad (19)$$

$$M_i \ddot{\Delta\omega}_i + D_i \dot{\Delta\omega}_i = P_i(t) - \sum_{j=1}^N K_{ij} \sin(\phi_i - \phi_j) + u_i(t), \quad (20)$$

Compared to the open-loop inertial Kuramoto model (19)–(20) without u_i , the reference-tracking controller introduces *additional tuning knobs* ($K_{p,i}, K_{i,i}$) that can accelerate convergence to $\Delta\omega_i = 0$ without modifying the physical parameters (M_i, D_i).

B. Reference-tracking PI control law

A PI controller on frequency deviation is now implemented as:

$$u_i(t) = -K_{p,i}\Delta\omega_i(t) - K_{i,i}z_i(t), \quad (21)$$

$$\dot{z}_i(t) = \Delta\omega_i(t), \quad (22)$$

where $K_{p,i} \geq 0$ provides fast proportional “frequency pull” and $K_{i,i} \geq 0$ eliminates steady-state frequency error via integral action. This structure is consistent with the notion that a globally shared reference allows K_p and K_i to act as active damping/stiffness knobs.

C. Step disturbance with power balance

Same step disturbance is applied to the mechanical power inputs at time t_0 :

$$P(t) = P_{\text{base}} + \mathbf{1}_{t \geq t_0} P_{\text{step}}, \quad (23)$$

where $\mathbf{1}_{t \geq t_0}$ is the unit-step indicator.

Again power balance is enforced:

$$\mathbf{1}^\top P_{\text{base}} = 0, \quad \mathbf{1}^\top P_{\text{step}} = 0, \quad (24)$$

where the second constraint is implemented by removing the mean of the injected step vector.

D. Equilibrium-consistent initial conditions

To initiate the simulation from a synchronized operating point (a “flat start” in frequency), we set the initial frequency deviation and controller state vectors to zero:

$$\Delta\omega(0) = \mathbf{0}, \quad z(0) = \mathbf{0}. \quad (25)$$

The initial phase angle vector $\phi(0) = \phi_0$ is computed as the steady-state solution to the power-balance equations under the baseline mechanical power P_{base} :

$$P_{\text{base},i} - \sum_{j=1}^N K_{ij} \sin(\phi_{0,i} - \phi_{0,j}) = 0, \quad i = 1, \dots, N. \quad (26)$$

This system is solved numerically using the `fsolve` algorithm to ensure that $\dot{\Delta\omega}(0) = \mathbf{0}$, thereby isolating the system’s pure transient response to the subsequent step disturbance.

E. Reference-tracking PI control law with Washout Filter

To ensure that the control effort $u_i(t)$ provides transient damping without altering the long-term steady-state power-flow equilibrium, a washout filter is applied to the integrator state:

$$u_i(t) = -K_{p,i}\Delta\omega_i(t) - K_{i,i}z_i(t), \quad (27)$$

$$\dot{z}_i(t) = \Delta\omega_i(t) - \frac{1}{\tau}z_i(t), \quad (28)$$

where $\tau > 0$ represents the washout time constant.

F. Steady-State Consistency

In the steady state, the system reaches a synchronized frequency where $\Delta\omega_i = 0$ and $\dot{z}_i = 0$. Substituting these conditions into (28) yields $z_i = 0$, which consequently forces the control torque to vanish:

$$\lim_{t \rightarrow \infty} u_i(t) = 0. \quad (29)$$

As $u_i(t)$ converges to zero, the closed-loop swing equation reduces to the natural power-balance requirement:

$$P_i(t) - \sum_{j=1}^N K_{ij} \sin(\phi_i - \phi_j) = 0. \quad (30)$$

This confirms that while the controller eliminates oscillatory transients, the final power sharing is determined solely by the physical network topology.

VI. SIMULATION RESULTS AND DISCUSSION

The natural open-loop response against the closed-loop reference-tracking controller equipped with the washout filter is now simulated and compared. The parameters used for the simulations are provided in Table I.

TABLE I
SIMULATION PARAMETERS FOR THE 3-GENERATOR INERTIAL KURAMOTO NETWORK

Category	Parameter	Value
Network	Number of generators N	3
Dynamics	Inertia constants M_i	[2.0, 3.0, 2.5]
	Damping coefficients D_i	[3.0, 3.0, 3.0]
Coupling	Coupling gain K_0	8.0
	Coupling matrix K_{ij}	$K_0(1 - \delta_{ij})$
Control	Proportional gains $K_{p,i}$	[8.0, 4.0, 3.0]
	Integral gains $K_{i,i}$	[4.0, 2.0, 1.0]
	Washout time constant τ	1.0 s
Disturbance	Baseline mechanical power P_{base}	[0.6, -0.3, -0.3]
	Step magnitude ΔP	2.0
	Step time t_0	3.0 s
Initialization	Initial frequency deviation	$\Delta\omega_i(0) = 0$
	Initial washout state	$z_i(0) = 0$
	Initial angles	Solved via <code>fsolve</code>

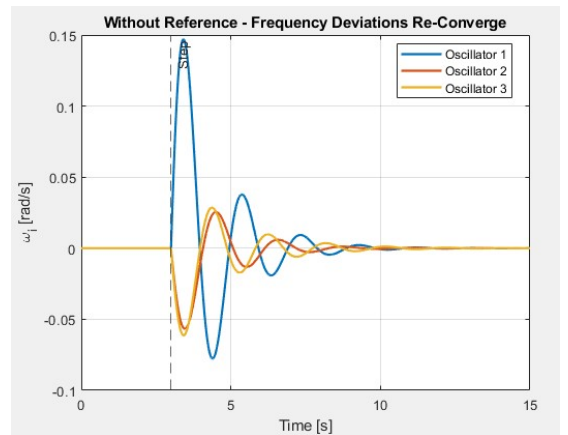


Fig. 1. Transient frequency deviations of a three-oscillator network without global frequency reference tracking. After a step disturbance, frequency restoration relies exclusively on network coupling, leading to pronounced oscillatory behavior.

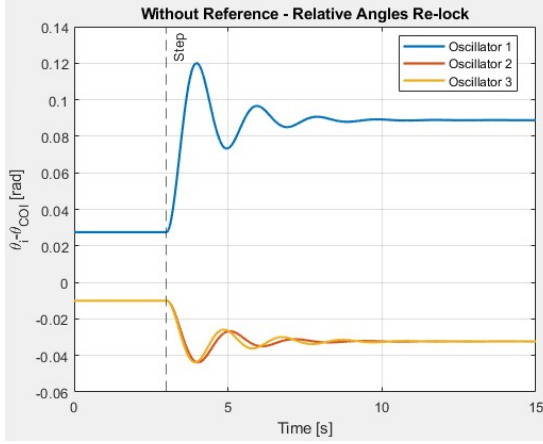


Fig. 2. Relative phase angles of the three oscillators without a global frequency reference. Following the disturbance, the oscillators re-lock through network coupling, and the steady-state phase offsets encode the resulting power-sharing equilibrium.

TABLE II
STEADY-STATE POWER SHARING VERIFICATION: NATURAL CASE (NO REFERENCE)

Osc.	P_m (pu)	P_e (pu)	Error
1	1.9333	1.9332	1.0×10^{-4}
2	-0.96667	-0.96698	3.1×10^{-4}
3	-0.96667	-0.96624	-4.3×10^{-4}
Total Sum	0.00000	0.00000	—

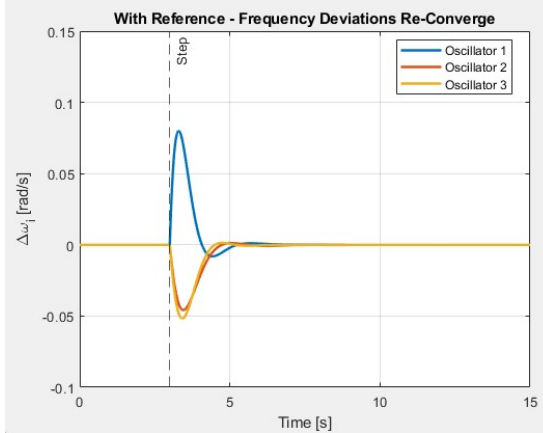


Fig. 3. Frequency deviations with global reference-frequency tracking. Following the disturbance, all oscillators rapidly re-converge to the reference frequency with strongly damped transients.

TABLE III
STEADY-STATE POWER SHARING VERIFICATION: REFERENCE-TRACKING CONTROLLER CASE

Osc.	P_m (pu)	Control effort u (pu)	P_e (pu)	Error
1	1.9333	-5.92×10^{-6}	1.9333	0.0000
2	-0.96667	4.32×10^{-6}	-0.96666	0.0000
3	-0.96667	1.59×10^{-6}	-0.96667	0.0000

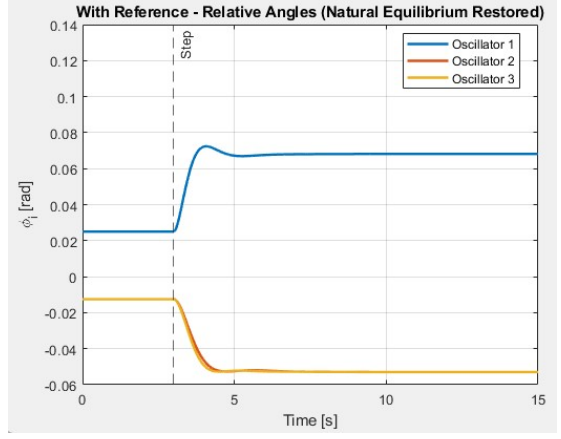


Fig. 4. With reference. Relative phase angles of the three oscillators under global reference-frequency tracking. After the disturbance, the washout mechanism restores the natural equilibrium, and the steady-state phase offsets encode the network-determined power sharing.

A. Transient Stability and Oscillation Suppression

The frequency deviation dynamics under a 2.0 pu step disturbance are illustrated in Fig. 1 and Fig. 3.

- **Overshoot Reduction:** In the natural case (Fig. 1), the system exhibits a peak frequency deviation of approximately 0.15 rad/s. In contrast, the reference-tracking architecture (Fig. 3) limits this overshoot to less than 0.08 rad/s, representing a nearly 50% improvement in transient frequency stability.
- **Damping Performance:** The open-loop system relies solely on network coupling and inherent damping D_i , leading to prolonged oscillations that persist for over 10 seconds. The proposed controller provides active damping via the K_p and K_i knobs, pulling frequency deviations to zero within 5 seconds with virtually no secondary ringing.

B. Phase Dynamics and Equilibrium Consistency

The evolution of relative phase angles is shown in Fig. 2 and Fig. 4.

- **Non-Oscillatory Locking:** The natural phase response is characterized by large underdamped swings before settling. The reference-tracking case exhibits a smooth, monotonic transition to the new synchronized state, which shows significant reduction in the stress on the converters and on the transmission lines possible.
- **Equilibrium Alignment:** Although the transient paths differ, the final angular separation between the leading oscillator (Osc. 1) and the lagging oscillators (Osc. 2, 3) is identical in both scenarios (≈ 0.120 rad).

C. Numerical Validation of Power Sharing

Numerical verification of the steady-state power balance is provided in Table II and Table III. Table III shows that the steady-state control effort u is effectively eliminated by the washout mechanism, reaching negligible values on the order of 10^{-6} pu. As a result of $u \rightarrow 0$, the electrical power export P_e matches the mechanical input P_m exactly.

VII. CONCLUSION

This paper studied oscillation suppression in grid-forming/VSM-type synchronization using a second-order Kuramoto (swing-network) model. In the conventional setting without an explicit global reference, frequency restoration and phase re-locking occur solely through network coupling, which leads to underdamped transients and large angular excursions following disturbances.

Assuming that the aggregate active-power balance is maintained, we proposed a primary-control augmentation in which all units track a broadcast global frequency reference via a simple PI loop acting on frequency deviation. The resulting closed-loop dynamics transform synchronization from mutual oscillator locking into a reference-tracking problem, yielding substantially improved transient behavior. Simulation results on a three-oscillator network showed reduced frequency overshoot, faster settling, and the elimination of underdamped ringing compared to the natural (open-loop) response.

REFERENCES

- [1] Zhang and R. Preece, "Effects of Droop Based Fast Frequency Response on Rotor Angle Stability During System Wide Active Power Deficits," in IEEE Transactions on Power Systems, vol. 39, no. 5, pp. 6578-6591, Sept. 2024, doi: 10.1109/TPWRS.2024.3364532.
- [2] T. X. Zhu, "Detection and Characterization of Oscillatory Transients Using Matching Pursuits With a Damped Sinusoidal Dictionary," in IEEE Transactions on Power Delivery, vol. 22, no. 2, pp. 1093-1099, April 2007, doi: 10.1109/TPWRD.2007.893451.
- [3] W. R. Lachs, "A New Transient Stability Control," in IEEE Transactions on Power Systems, vol. 2, no. 4, pp. 980-986, Nov. 1987, doi: 10.1109/TPWRS.1987.4335289.
- [4] L. Fan, Z. Miao and Z. Wang, "A New Type of Weak Grid IBR Oscillations," in IEEE Transactions on Power Systems, vol. 38, no. 1, pp. 988-991, Jan. 2023, doi: 10.1109/TPWRS.2022.3220050.
- [5] F. Guo, C. Wen, J. Mao and Y. -D. Song, "Distributed Secondary Voltage and Frequency Restoration Control of Droop-Controlled Inverter-Based Microgrids," in IEEE Transactions on Industrial Electronics,
- [6] H. Huang, F. Li and Y. Mishra, "Modeling Dynamic Demand Response Using Monte Carlo Simulation and Interval Mathematics for Boundary Estimation," in IEEE Transactions on Smart Grid, vol. 6, no. 6, pp. 2704-2713, Nov. 2015, doi: 10.1109/TSG.2015.2435011.
- [7] H. Asadi, S. Mohamed and S. Nahavandi, "Incorporating Human Perception With the Motion Washout Filter Using Fuzzy Logic Control," in IEEE/ASME Transactions on Mechatronics, vol. 20, no. 6, pp. 3276-3284, Dec. 2015, doi: 10.1109/TMECH.2015.2405934.
- [8] B. Alghamdi and C. A. Cañizares, "Frequency Regulation in Isolated Microgrids Through Optimal Droop Gain and Voltage Control," in IEEE Transactions on Smart Grid, vol. 12, no. 2, pp. 988-998, March 2021.
- [9] X. Meng, J. Liu and Z. Liu, "A Generalized Droop Control for Grid-Supporting Inverter Based on Comparison Between Traditional Droop Control and Virtual Synchronous Generator Control," in IEEE Transactions on Power Electronics, vol. 34, no. 6, pp. 5416-5438, June 2019, doi: 10.1109/TPEL.2018.2868722.
- [10] D. Groß, M. Colombino, J. -S. Brouillon and F. Dörfler, "The Effect of Transmission-Line Dynamics on Grid-Forming Dispatchable Virtual Oscillator Control," in IEEE Transactions on Control of Network Systems, vol. 6, no. 3, pp. 1148-1160, Sept. 2019, doi: 10.1109/TCNS.2019.2921347.
- [11] MATLAB, Version R2024b, The MathWorks, Inc., Natick, MA, USA, 2024.